Proceedings of the SEM Annual Conference
June 1-4, 2009 Albuquerque New Mexico USA

Deformation and Failure of Polycarbonate during Impact as a Function of Thickness

C. Allan Gunnarsson
allan.gunnarsson@arl.army.mil

Benjamin Ziemski

Tusit Weerasooriya
tusitw@arl.army.mil

Paul Moy
pmoy@arl.army.mil

Army Research Laboratory
Weapons and Materials Directorate
Bldg 4600 Deer Creek Loop
Aberdeen Proving Ground, MD 21005-5069

ABSTRACT
Polycarbonate (PC) is a commonly used thermoplastic for transparent protection. This thermoplastic is subjected to many forms of impact and it is important to understand the deformation behavior of this material under impact conditions. In this study, blunt impact experiments were conducted on polycarbonate panels of varying thicknesses and configurations. During impact, two high-speed cameras recorded digital images of a speckle pattern on the back surface. These images were post processed using digital image correlation technique to obtain the full-field deformation measurements including out-of-plane displacement. In this paper, experimental results are presented as a function of velocity and thickness of the panels.

INTRODUCTION
Amorphous glassy polymers have been widely used for many structural applications in the aerospace and automotive industry due to its transparency, low density, and, in particular, high impact strength. Polycarbonate (PC) is a thermoplastic polymer that is easily molded and thermoformed. This is due in part to the low glass transition temperature (T_g) of 150°C [1-2]. The glass transition temperature is the temperature at which an amorphous solid, such as glass or a polymer, becomes brittle on cooling, or soft on heating [3]. PC is impact resistant and transparent; even though it is relatively soft and susceptible for scratching, the impact characteristics make it ideal for transparent protection against dynamic loading in applications, such as in vehicle windows, where visibility is required.

PC has been extensively investigated over the past decades for its toughness, tensile, and compressive strengths, however, the mechanical response and failure behavior at high strain rates are still not completely understood. The mechanical properties of polymers are dependent upon two key factors, the rate of deformation and temperature. Polymers, tested at high rates of strain, typically have an increase of the yield strength and the modulus and a decrease in strain to failure when compared to quasi-static results [4, 5].

The work by Moy et al [6] showed that PC is rate sensitive under uniaxial compression. Their research indicates a softening after yielding, followed by a strain hardening phase at low and high strain rates. Mulliken et al [7] reported similar behavior of PC at high strain rates. Their work also included DMA analyses for PC, as well as PMMA, to characterize the viscoelastic behavior for these thermoplastics. Another polymer study by Hall [8] reports that the temperature increases during deformation at high strain rate, whereas no temperature change at lower rates. Work by Walley et al [9] has shown that the strain rate and temperature affects the strain hardening behavior of glassy polymers. Material models by Arruda et al [10] and Boyce et al [11, 12] for both PC and PMMA have been proposed to predict the trend for differing strain rates.

Research efforts to obtain the constitutive behavior of polycarbonate experimentally and the development of material models for this polymer are well documented. However, the validation of material models requires different types of experimental data. The model development and validation depend on the availability of experimental data. Therefore, as a compliment to modeling efforts related to impact, an experimental technique was developed to obtain quantitative data under impact loading conditions for PC panels by Gunnarsson et al [13]. This type of data is essential for validation or refinement of the transient deformation and, eventually, failure prediction produced by models. The impact experiments conducted in this report utilize digital image correlation (DIC) as the primary method of instrumentation and measurement [15-19]. DIC is a non-contact, optical technique that tracks the surface deformation of an object. This method provides full-field as well as out-of-plane measurements.

For DIC, a speckle-like pattern is directly applied to the surface of the sample. The pattern is typically produced by using consumer spray paint of black and white, which offers the best contrast for the monochromatic cameras that were used for the impact experiments. Two high-speed digital cameras, in a stereoscopic setup, captured the deformation of the speckled surface. Thus, the dual camera setup provides images for out-of-plane measurements. The DIC method allows the authors to obtain deformation data at a much higher resolution than previous methods, such as Shadow-Moiré method used in a previous impact study on composite panels by Weerasooriya [14].

The algorithms in the DIC software determine the surface displacement and deformation of an object by tracking the gray scale pixel array that is generated from the high contrast (black-white) speckle pattern in each picture. This is done through post-processing of the captured images. The software allows highly detailed images of the displacement and strain fields. The ability to acquire the full-field measurement at the impact zone and surrounding area provides detailed data to compare with results from computer simulations using different material models. Two key features that make the DIC technique so unique are its high accuracy (approximately 50μ strain), and the ability to account for the rigid body movement of the object. Additionally, sample preparation is non-intrusive, particularly significant when working with polymers.

This work extends previous work conducted to study the impact on panels of one thickness to study the back surface behavior of PC panels during impact as a function of thickness. Also, the penetration threshold of PC is studied as a function of thickness. Impact velocity is incrementally changed until penetration is achieved, thus giving the impact energy of the projectile needed for penetration for a certain thickness and impactor geometry. The measured full-field displacement results are presented in this paper as well as penetration data.

MATERIAL

The PC panels were acquired from Sabic Polymer-Shapes (Jessup, Maryland). The size of each panel was 305 mm by 305 mm (12 in by 12 in). PC panels of five different thicknesses were used for impact experiments. The nominal physical properties from the manufacturer are given below in Table 1.

Table 1. Nominal Properties of Polycarbonate

Density (kg/m^3)	1200
Tensile Modulus (MPa)	2350
Yield Stress (MPa)	63
Yield Strain (%)	5.8
UTS (MPa)	55

EXPERIMENTAL PROCEDURE

Target Preparation

The speckle pattern required for DIC was created on the PC panels by spray painting one side of the panel surface completely white and then adding random black dots (or speckles) by using a coarse applicator of black spray paint. A PC panel with applied speckle pattern is shown in Figure 1.

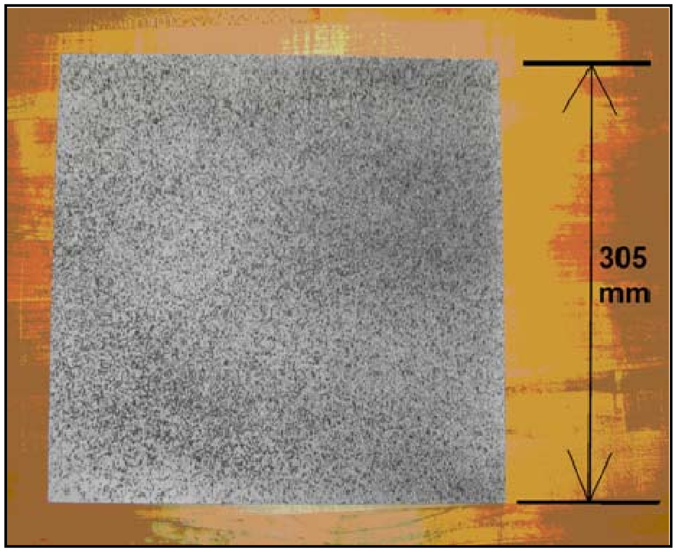

Figure 1. PC Panel with Speckle Pattern for DIC

Mounting

During impact experiments, the PC panels were clamped between an aluminum mounting frame and an aluminum support. The aluminum support increased distribution of the clamping force along the perimeter of the panel. The frame and the support had outside dimensions identical to the PC targets and were 25.4 mm thick, providing a 254 mm by 254 mm area of the target exposed to the camera. The mounting system of the target is shown in Figure 2(a). A large enclosure was used to safely contain the projectile during penetration testing. This can be seen in Figure 2(b).

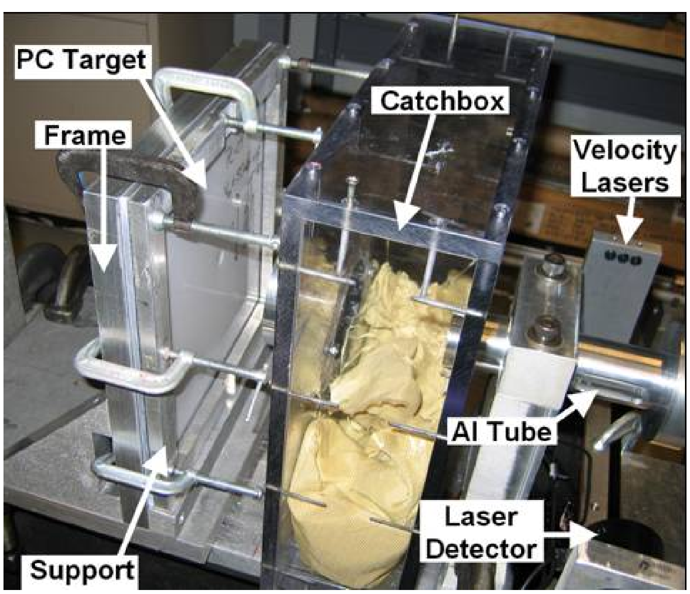

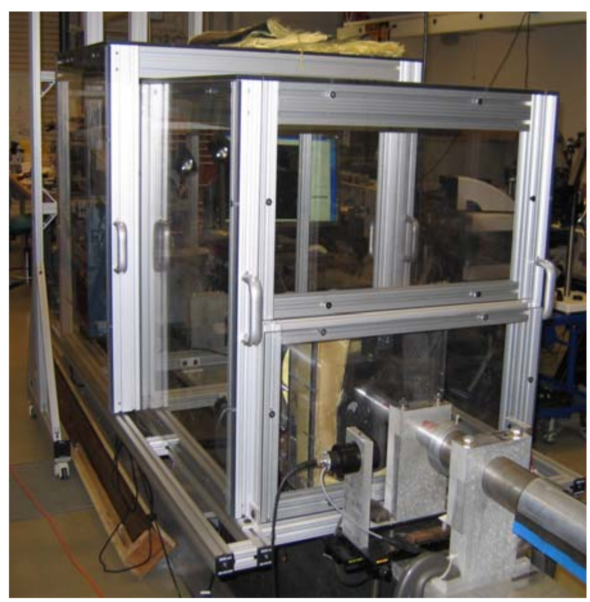

Figure 2. (a) PC Panel Mounting Setup for Impact Experiment and (b) Large Safety Enclosure

Projectile

The impact experiments were conducted using a gas gun with a 25.4 mm (1.0 in) diameter bore. The projectile was made of Maraging 350 steel inserted into an acrylic sabot; total projectile mass (including sabot) was 104 grams. The impact end of the steel projectile was hemispherical in shape, with a radius of 6.35 mm. The detailed geometry of the projectile can be seen in Figure 3. Dimensions in the CAD drawing are in inches.

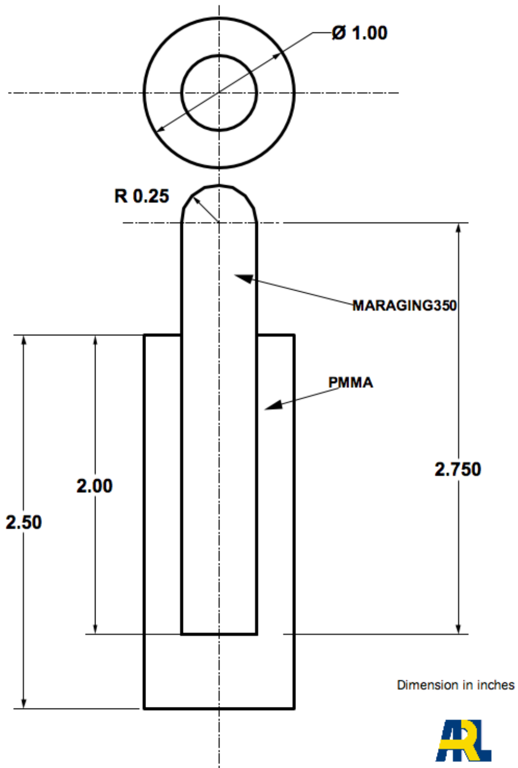

Figure 3. Maraging 350 Steel Hemispherical-Nosed Projectile (dimensions are inches)

An inert gas (N_2) filled breech is used to propel the projectile through the gun tube. The gas gun is fired remotely, using a fast acting (120 ms close to open time) solenoid valve. The projectile exited the gun tube, passed through an aluminum tube and catch box, before impact on the PC panel. During DIC testing, the projectile does not penetrate the target and bounces off the target into the catch-box. To determine the penetration velocity, the projectile would penetrate the target and then encounter a secondary catch box filled with unpacked Kevlar to stop it. The projectile impact path is normal to the panel. Initially, experiments were conducted to obtain the velocity required for penetration of 3.00, 4.45 and 5.85 mm thick panels. This allowed selection of test velocities for DIC testing that were well below the penetration values. The target panels were aligned so that the impact point is at the center of the square using a targeting laser inserted into the gun bore. DIC experiments were performed on PC targets of the following thicknesses: 3.00, 4.45, 5.85, 9.27, and 12.32 mm.

Velocity Measurement

Three lasers positioned sequentially determined the projectile velocity during these impact experiments. The aluminum tube, attached at the outlet of the gas gun barrel, protects the laser setup from inadvertent damage during the impact experiments. Three small holes in the tube permitted the laser beams to pass through, as shown in Figure 4, to the detector on the opposite side. An interruption of the first laser beam by the projectile produced a change in voltage being produced by the detector. As the three laser beams are interrupted by the projectile, a four step voltage trace is recorded by a digital oscilloscope. The time between the step changes was the travel time of the projectile between each laser. The distances between the lasers were measured and then used with the time data to determine velocity. The oscilloscope in the laser velocity measuring system also acts as the trigger mechanism for the high-speed digital cameras. When the oscilloscope is triggered by the interruption of the first laser beam, the oscilloscope is configured to send a TTL pulse to trigger recording by the high-speed digital cameras.

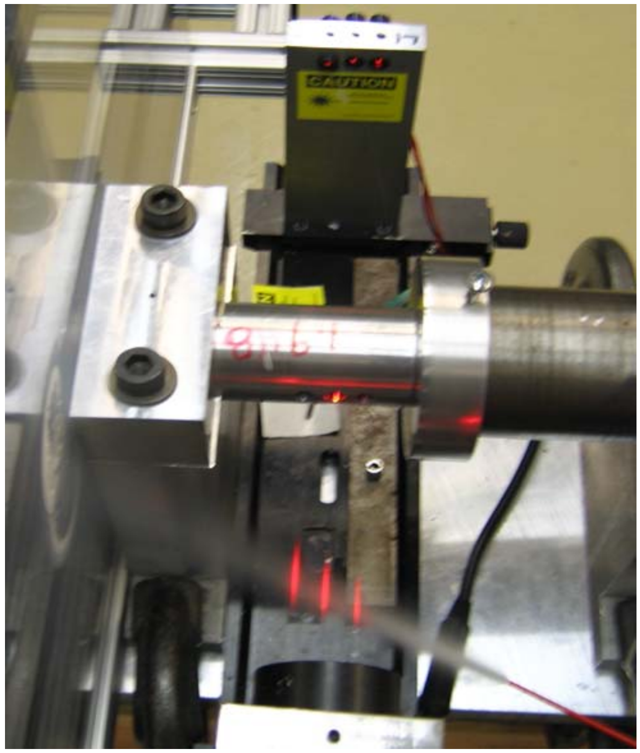

Figure 4. Laser Velocity Measurement Setup

DIC Measurement

The DIC system used in the impact experiments consisted of two Photron APX-RS high-speed digital cameras connected to a Windows-based computer. The proprietary Photron camera software was used to set-up the cameras and retrieve the back surface images of the PC after impact. After testing, the images from the cameras were post-processed using commercial DIC software from Correlated Solutions Inc. to obtain the three dimensional displacement data of the back-surface of the PC panel. The cameras were setup to record at a frame rate of 30,000 frames per second. This frame rate permitted a maximum resolution of 256 by 256 pixels for the camera images, which was utilized.

The necessary physical attributes of the cameras, such as focal length and relative position, were determined using the built in calibration feature of the DIC software by capturing several dozen pictures of a special calibration grid. After inputting the grid properties, such as grid spacing and size, the software calculated the attributes. Once calibrated, the software analyzed the speckle pattern present in the area of interest of every picture and calculated the full-field displacement, deformation, and strains (ε_{xx}, ε_{yy}, ε_{xy}, and, ε_1 and ε_2). A schematic of the data acquisition setup with the DIC cameras is depicted in Figure 5.

The camera parameters were configured for a frame rate of 30,000 frames per second (fps) at a resolution of 256 by 256 pixels. This provided a good balance between image resolution within the field of view and the number of frames needed to record the relevant impact event. The exposure time was set to the maximum available to allow as much light as possible for the cameras. Sufficient lighting levels were achieved using a light stand that consisted of eight 250W halogen bulbs.

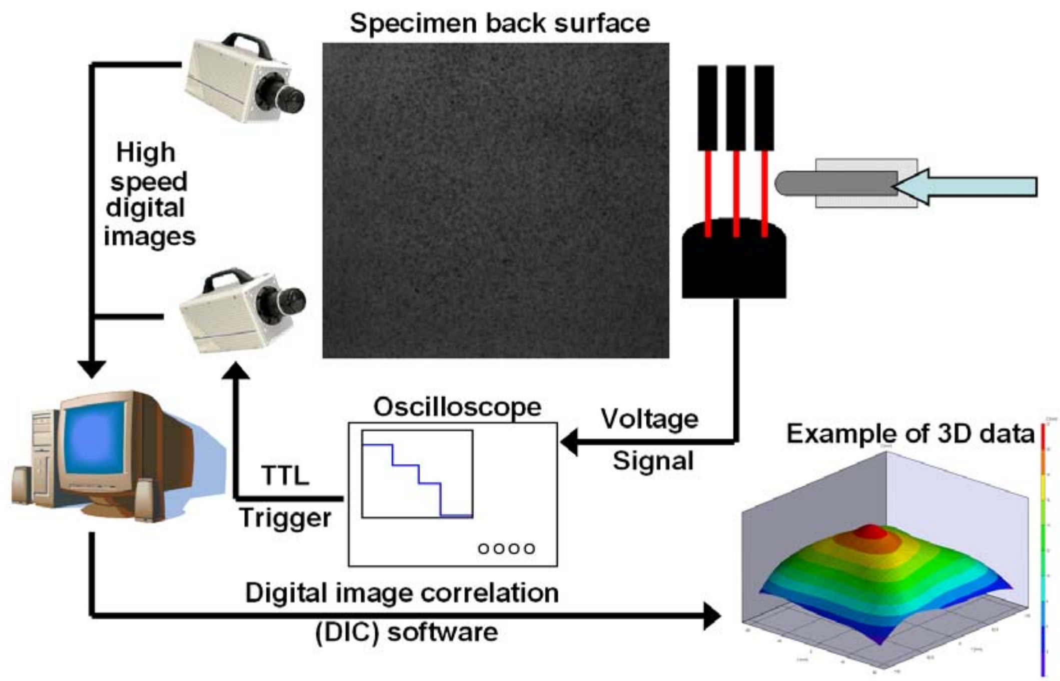

Figure 5. Schematic of Impact Setup using DIC for Back Surface Measurements

RESULTS AND DISCUSSION

Experiments were conducted on 3.00, 4.45 and 5.85 mm thick panels to obtain the velocity required for penetration. Table 2 shows the results from these experiments. Based on these experiments, velocities were selected for non-penetration experiments for full-field back surface measurements. The penetration velocity and energy are shown below as a function of thickness in Figure 6.

Table 2 – Summary of Penetration Data

Thickness = 3.00 mm		Thickness = 4.45 mm		Thickness = 5.85 mm	
Impact Velocity (m/s)	Penetration (Y/N)	Impact Velocity (m/s)	Penetration (Y/N)	Impact Velocity (m/s)	Penetration (Y/N)
104.4	Y	81.2	Y	68.3	Y
96.4	Y	72.0	Y	64.0	Y
90.0	Y	70.6	N	63.2	N
86.3	Y	67.6	N	61.5	N
81.2	Y	60.7	N	60.2	N
79.5	N	50.1	N		
77.5	N				

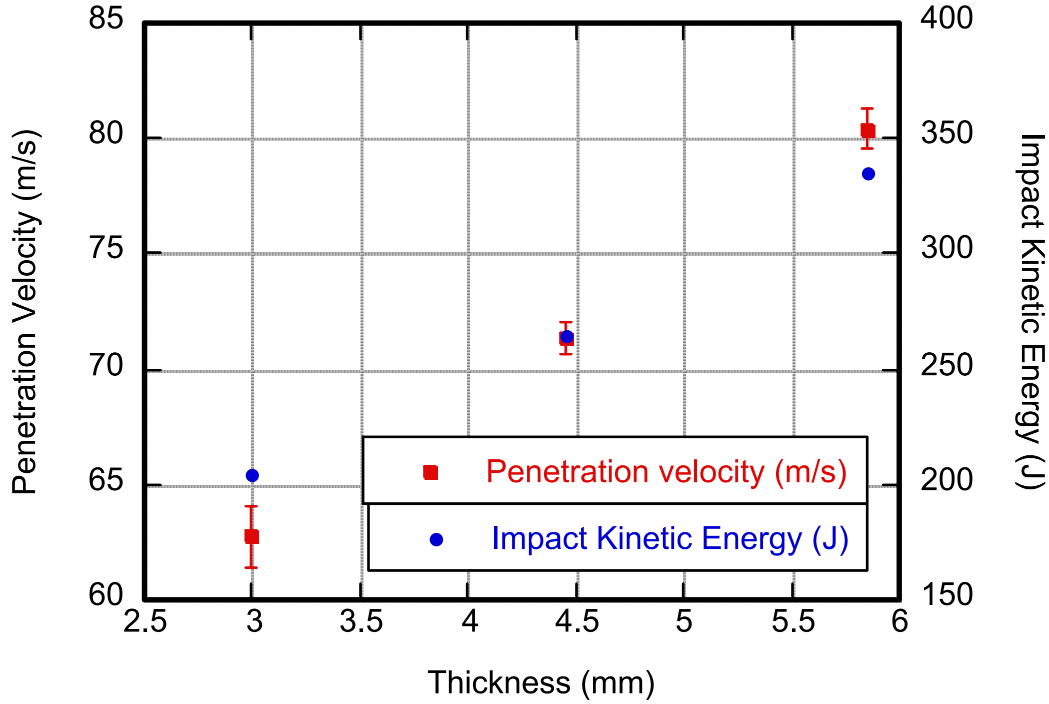

Figure 6. Penetration Velocity and Impactor Kinetic Energy for Penetration as a Function of Panel Thickness

The transient deformation data generated by the DIC was used to determine how the PC behaved during the blunt impact. The DIC data is presented both graphically and numerically. The full field 2-D and 3-D contour plots for the impact velocity experiment at 50 m/s for the 5.85 mm thick PC are shown below in Figure 7(a) and 7(b), respectively. Both contour plots show the maximum out-of-plane displacement (z-direction) at the time 1.3 ms after impact. The 2D full-field is overlaid with the corresponding deformed image whereas the 3-D contour is displayed on an x-y-z coordinate axes plot. The 3-D surface map is equivalent to same dimensional area as the 2-D overlay and not a full representation of the entire PC panel. The z-scale is not proportional to the x-y axes and thus the exaggerated profile in the z-direction. The graphical representations shown are typical of the data acquired for all of the experiments performed.

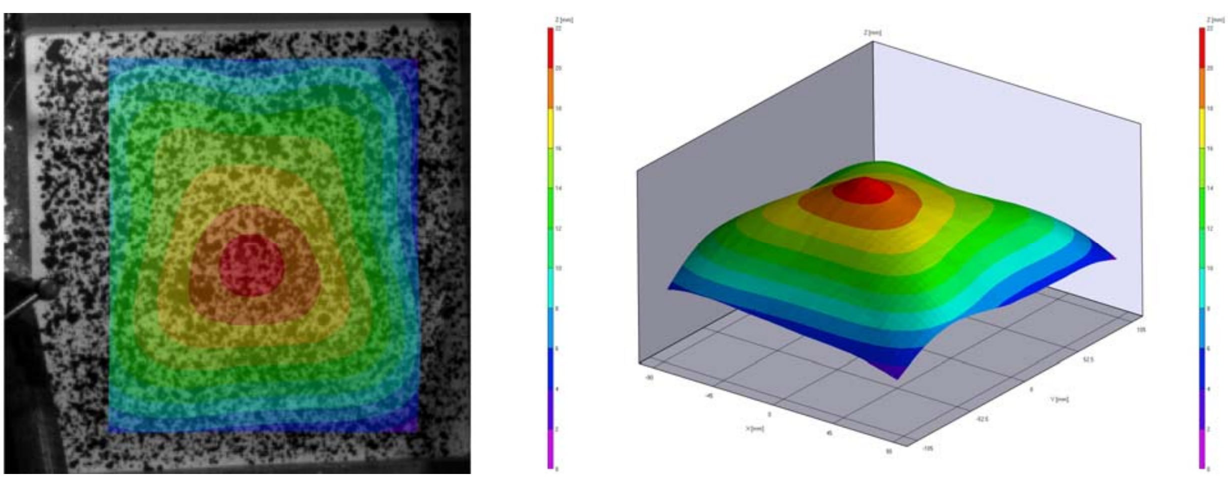

(a) (b)

Figure 7. (a) 2-D and (b) 3-D Contour Plots for 5.85 mm Thick PC at Velocity of 50.6 m/s at Displacement Maximum (1.3 ms after impact)

Numerical data was then extracted from these graphical data. Shown in the proceeding sections are plots of the out-of-plane displacement as a function of time for the impact point for the different thicknesses and velocities. In all of these, time of zero ms corresponds to the beginning of the impact. Unfortunately, for both the 3.00 mm and 4.45 mm thick panels, the paint speckle pattern de-bonded from the panel at impact velocity of approximately 30 m/s. That is the reason for only two velocity data for those two thicknesses. The maximum displacements at the impact point for each velocity and thickness are tabulated below in Table 3. The maximum displacement values were extracted from the correlated data at the location of impact (panel center).

Table 3. Maximum Displacements at the Impact Point for Different Impact Velocities and Panel Thicknesses

Thickness (mm)	Approximate Impact Velocity (m/s)				
	10	20	30	40	50
	Maximum Displacement (mm)				
3.00	13.2	16.1	-	-	-
4.45	9.4	12.9	-	-	-
5.85	6.5	10.9	15.2	19.2	22
9.27	-	-	10.2	11.3	14.0
12.32	-	-	6.9	8.7	10.7

Figure 8 shows the out of plane displacement at the impact point for 3.0 mm thick plates for impact velocities of 12 and 19 m/s. Maximum displacements for the 12 m/s and 19 m/s velocities are 13.2 and 19.0 mm, respectively.

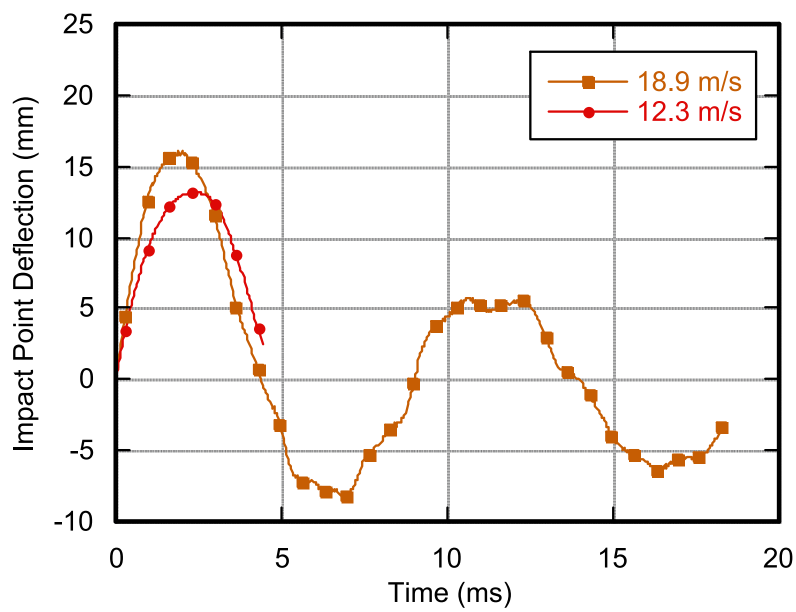

Figure 8. Z-Displacement for 3.00 mm thick PC Panels for Velocities 12 and 19 m/s.

Figure 9 shows the response of the 4.45 mm PC panel for impact velocities of 10 and 19 m/s. At 10 m/s impact, maximum displacement at the impact point is 9.4 mm. For the same panel at 19 m/s velocity, the maximum displacement at the impact point is 12.9 mm.

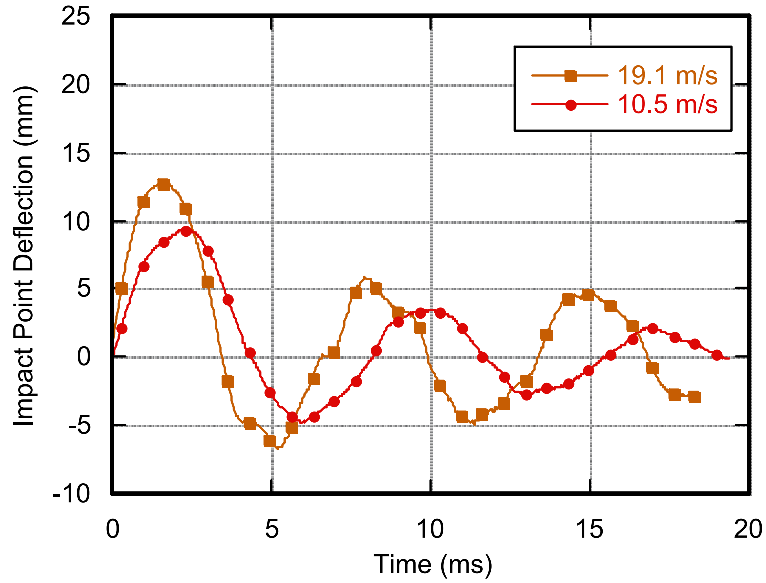

Figure 9. Z-Displacement for 4.45 mm thick PC Panels for Velocities 11 and 19 m/s.

Figure 10 shows the response of the 5.85 mm thick PC panels for five different impact velocities. For this thickness panel, for the impact velocities of 11, 19, 31, 41 and 51 m/s, the maximum out-of-plane displacements at the impact point are 6.5, 10.9, 15.2, 19.2 and 22 mm, respectively.

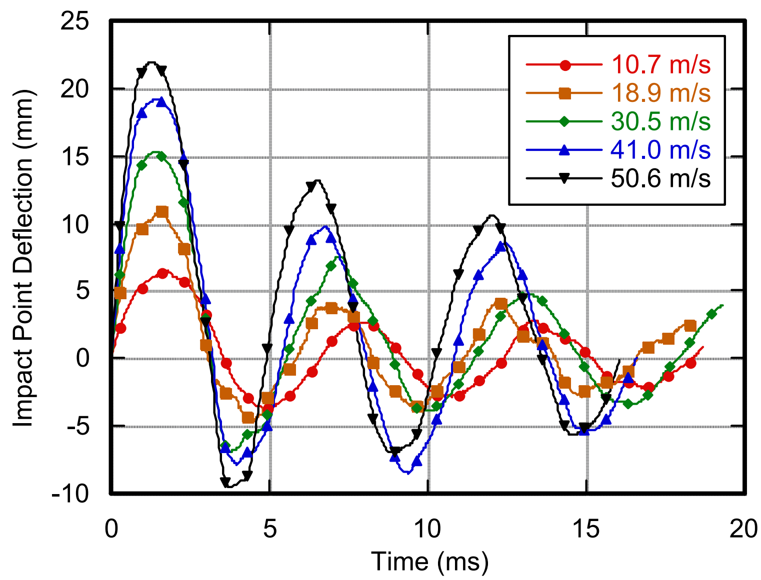

Figure 10. Z-Displacement for 5.85 mm thick PC Panels for Velocities 11, 19, 31, 41, and 51 m/s.

Figure 11 shows the response of 9.27 mm thick PC panels for three different impact velocities. For this thickness, the impact velocities are 31, 38, and 48 m/s and the respective maximum displacements are 10.2, 11.3, and 14.0 mm.

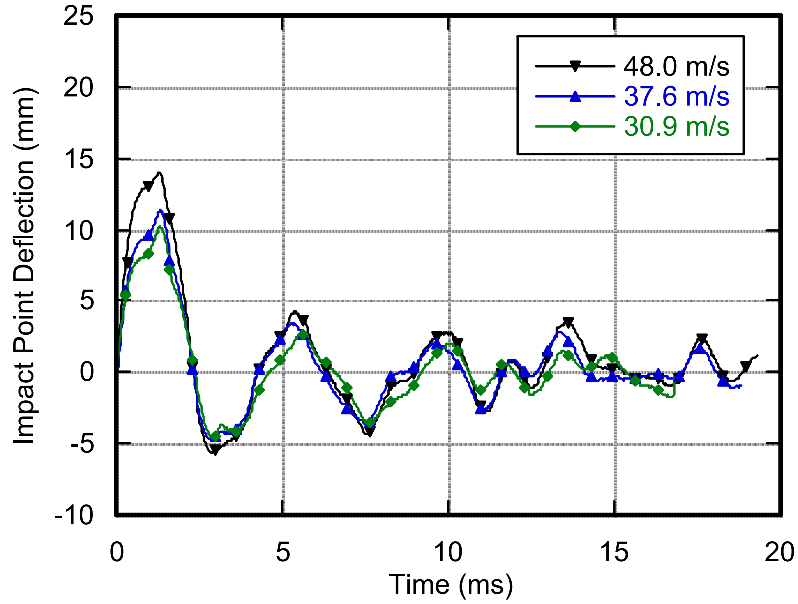

Figure 11. Z-Displacement for 9.27 mm thick PC Panels for Velocities 31, 38, and 48 m/s.

The impact response for 12.3 mm thick PC is shown in Figure 12. For the panel of 12.3 mm thickness, maximum displacements at the impact point are 6.9, 8.7 and 10.7 mm for impact velocities of 30, 41 and 49 m/s.

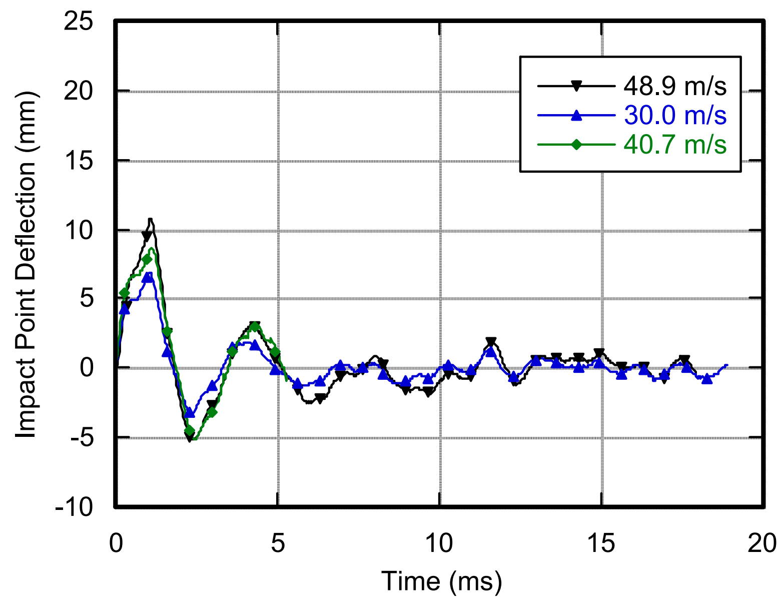

Figure 12. Z-Displacement for 12.32 mm thick PC Panels for Velocities 30, 41, and 49 m/s.

Maximum impact-point displacement as a function of impact velocity is given in Figure 13 for all the thicknesses of the PC panels.

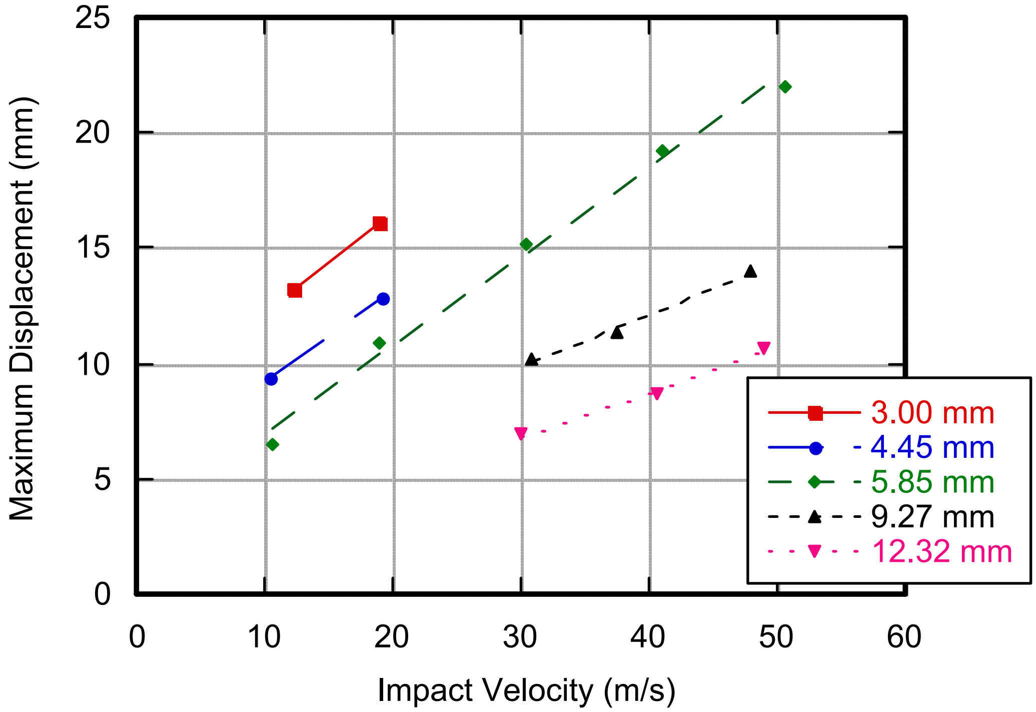

Figure 13. Maximum Displacement vs. Impact velocity as a Function of Panel Thickness

For a given thickness, maximum displacement increases with the impact velocity for all PC panels. As the panel thickness increases, the effect of impact velocity changes on the maximum displacement decreases. From the graph, it can be seen that for the 5.85, 9.27, and 12.32 mm thicknesses, the maximum displacement is linearly related to changes in the impact velocity. There is not enough data for the two smaller thicknesses to identify such a trend.

SUMMARY

The blunt impact response of PC at low velocities was obtained. A technique and setup was developed to determine the velocity required for penetration as a function of panel thickness for this penetrator with PC. The experimental methodology was developed to conduct non-penetrating blunt impact tests on PC panels with a thickness of up to 12.3 mm. Full-field out-of-plane transient displacements were measured during impact using DIC. Several elements, such as safety enclosure setup, lighting, speckle pattern application, high speed camera set-up, and velocity measurement, were refined for this particular application. Back surface displacements were determined from the data using the DIC technique. The data from these experiments can be used to evaluate and refine material models and computational methodologies that are used to predict the impact response of PC. To compliment this effort, additional impact experiments for PC will be performed to obtain impact response using DIC during penetration as well as the response against different projectiles (mass and nose tip).

ACKNOWLEDGEMENTS

The authors would like to acknowledge colleague, Dr. Parimal J. Patel, at the Army Research Laboratory for his assistance in providing the technical knowledge and the PC panels used in this work.

Certain commercial equipment and materials are identified in this paper in order to adequately specifiy the experimental procedure. In no case does such identification imply recommendation by the Army Research Laboratory nor does it imply that the material or equipment identified is necessarily the best available for this purpose.

REFERENCES

1. Myers, F.S. and Brittain, J.O. Mechanical Relaxation in Polycarbonate-Polysulfone Blends. Journal of Applied Polymer Science, 17, pp. 2715-2724. 1973.
2. Petersen, R.J., Corneliussen, R.D., and Rozelle, L.T. Polymer Reprint, 10, pp. 385. 1969.
3. The IUPAC Compendium of Chemical Terminology, 66th Ed., pg 583 (1997).
4. Lo, Y.C. and Halldin, G. W. The Effect of Strain Rate and Degree of Crystallinity on the Solid-Phase Flow Behavior of Thermoplastic. ANTEC '84, pp. 488-491. 1984
5. Kaufman, H. S. Introduction to Polymer Science and Technology. John Wiley and Sons Press, New York. 1977.
6. Moy, P, Weerasooriya, T., Hsieh, A. and Chen, W. Strain Rate Response of a Polycarbonate Under Uniaxial Compression. Proceedings of SEM Annual Conference on Experimental Mechanics. June 2003.
7. Mulliken, A. D. and Boyce, M. C. Mechanics of rate-dependent elastic-plastic deformation of glassy polymers from low to high strain rates. Int. J. Solids Struct. 43:5, pp. 1331–1356. 2006
8. Hall, I. H. The Effect of Strain Rate on the Stress-Strain Curve of Oriented Polymers. II. The Influence of Heat Developed During Extension. Journal of Applied Polymer Science, 12, pp 739. 1968.
9. Walley, S. M., Field, J. E., Pope, P. H., and Stafford, N. A. A Study of the Rapid Deformation Behavior of a Range of Polymers. Philos. Trans. Soc. London, A, 328, pp. 783-811. 1989.
10. Arruda, E. M., Boyce, M. C., and Jayachandran, R. Effects of Strain Rate, Temperature, and Thermomechanical Coupling on the Finite Strain Deformation of Glassy Polymers. Mechanics of Materials, 19, pp. 193-212. 1995
11. Boyce, M. C. Arruda, E. M., Jayachandran, R. The Large Strain Compression, Tension, and Simple Shear of Polycarbonate. Polymer Engineering and Science, Vol. 34, No. 9, pp. 716-725. 1994.
12. Boyce, M.C. and Sarva, S. S. Mechanics of Polycarbonate during High-rate Tension. Journal of Mechanics of Materials and Structures. Volume 2 Issue 10, pp. 1853-1880. December 2007.
13. Gunnarsson, C. A., Weerasooriya, T., and Moy, Paul. Measurement of Transient Full-Field, Out-of-Plane Back Surface Displacements of Polycarbonate during Impact. Proceedings of the 2008 International Congress and Exposition on Experimental Mechanics and Applied Mechanics. June 2008.
14. Weerasooriya, T. Full Field Out-of-Plane Transient Deformation for Several Composites on Impact. ARL Technical Report to be published.
15. Chu, T. C., Ranson, W. F., Sutton, M. A., and Peters, W. H. Applications of Digital-Image-Correlation Techniques to Experimental Mechanics. Experimental Mechanics. September 1995.
16. Sutton, M. A., Wolters, W. J., Peters, W. H., Ranson, W. F., and McNeill, S. R. Determination of Displacements Using an Improved Digital Image Correlation Method. Computer Vision. August 1983.
17. Bruck, H. A., McNeill, S. R., Russell S. S., Sutton, M. A. Use of Digital Image Correlation for Determination of Displacements and Strains. Non-Destructive Evaluation for Aerospace Requirements. 1989.
18. Sutton, M. A., McNeill, S. R., Helm, J. D., Schreier, H. Full-Field Non-Contacting Measurement of Surface Deformation on Planar or Curved Surfaces Using Advanced Vision Systems. Proceedings of the International Conference on Advanced Technology in Experimental Mechanics. July 1999.
19. Sutton, M. A., McNeill, S. R., Helm, and Chao, Y. J. Advances in Two-Dimensional and Three-Dimensional Computer Vision. Photomechanics. Volume 77. 2000.